

Article

Use of $\text{NaNO}_3/\text{SiAl}$ as Heterogeneous Catalyst for Fatty Acid Methyl Ester Production from Rapeseed Oil

José María Encinar ¹, Juan Félix González ², Gloria Martínez ¹ and Sergio Nogales-Delgado ^{1,*}

¹ Department of Chemical Engineering and Physical-Chemistry, University of Extremadura, Avda. de Elvas s/n, 06006 Badajoz, Spain; jencinar@unex.es (J.M.E.); gloria.martinez3@educa.madrid.org (G.M.)

² Department of Applied Physics, University of Extremadura, Avda. de Elvas s/n, 06006 Badajoz, Spain; jfelixgg@unex.es

* Correspondence: senogalesd@unex.es

Abstract: The use of heterogeneous catalysts to produce fatty acid methyl esters (FAME) through transesterification with methanol might contribute to both green chemistry and a circular economy, as the process can be simplified, not requiring additional stages to recover the catalyst once the reaction takes place. For this purpose, different catalysts are used, including a wide range of possibilities. In this research the use of $\text{NaNO}_3/\text{SiAl}$ as a heterogeneous catalyst for FAME production through transesterification of rapeseed oil with methanol is considered. A thorough characterization of the catalyst (including XDR and XPS analysis, SEM microscopy, lixiviation and reusability tests, among others), specific optimization of transesterification by using the final catalyst (considering catalyst amount, stirring rate, methanol/oil ratio, and temperature), and quality determination of the final biodiesel (following the UNE-EN 14214 standard) were carried out. In conclusion, $20 \text{ mmol}_{\text{Na}} \cdot \text{g}_{\text{support}}^{-1}$ (that is, $\text{NaNO}_3/\text{SiAl}$ 20/1) offered the best results, with a high activity (exceeding 99% *w/w* of FAMES) without requiring higher impregnation amounts. The best chemical conditions for this heterogeneous catalyst were 5% *w/w* catalyst, 700 rpm, 9:1 methanol/oil ratio, and 65 °C, obtaining $E_a = 73.3 \text{ kJ} \cdot \text{mol}^{-1}$ and a high-quality biodiesel, similar to those obtained through homogeneous catalysis. Consequently, this catalyst could be a suitable precursor for FAME production.

Keywords: biodiesel; scanning electron microscopy; X-ray diffraction; reusability; kinetic study



Citation: Encinar, J.M.; González, J.F.; Martínez, G.; Nogales-Delgado, S. Use of $\text{NaNO}_3/\text{SiAl}$ as Heterogeneous Catalyst for Fatty Acid Methyl Ester Production from Rapeseed Oil. *Catalysts* **2021**, *11*, 1405. <https://doi.org/10.3390/catal11111405>

Academic Editors: Sunyoung Park, Dae Sung Park and Ki Hyuk Kang

Received: 30 October 2021

Accepted: 17 November 2021

Published: 20 November 2021

Publisher's Note: MDPI stays neutral with regard to jurisdictional claims in published maps and institutional affiliations.



Copyright: © 2021 by the authors. Licensee MDPI, Basel, Switzerland. This article is an open access article distributed under the terms and conditions of the Creative Commons Attribution (CC BY) license (<https://creativecommons.org/licenses/by/4.0/>).

1. Introduction

Traditional biodiesel production through homogeneous catalysis produces fatty acid methyl esters (FAMEs), showing satisfactory results at relatively low temperatures and air pressure with short reaction times and low catalyst concentrations, especially for base catalysis. However, the main disadvantage related to this kind of catalysis is catalyst removal, normally through washing treatments, which implies an additional step. Additionally, the subsequent wastewater (acidic or alkaline, depending on the catalyst used) requires further treatment [1,2].

The use of heterogeneous catalysts could be an alternative, gaining more and more importance [3]. The increase in costs due to their use (related to the cost of materials, catalyst preparation, and more extreme chemical conditions) can be offset by their reusability and the subsequent sustainability of the process [3,4]. Moreover, the use of relatively abundant and cheap active phases (for instance, salts that can easily add metal species, such as NaNO_3) and supports (such as SiAl) could improve the efficiency of the process. Consequently, biodiesel could represent a feasible alternative for diesel from an economic point of view.

In heterogeneous catalysis, the chemical reaction takes place on the surface of the catalyst, and the previous adsorption of the reagents is necessary, followed by the final desorption of the evolved products. Regarding transesterification of triglycerides, the

most accepted reaction mechanisms (as they properly reproduce experimental results) are Eley-Rideal (ER) [5,6] and Langmuir-Hinshelwood (LH) mechanisms [6,7].

When heterogeneous catalysts with basic properties are used, the ER mechanism proposes that the alcohol is adsorbed in basic sites of the solid, so that the methoxide group on the catalyst's surface reacts with the carbonyl group of the triglyceride, which is in a liquid phase. Thus, there are four stages: methanol adsorption, reaction in catalyst's surface (where a tetrahedral intermediate between the methoxide group and the triglyceride will be generated), fatty acid methyl ester release, and glyceride desorption (diglyceride, monoglyceride, or glycerol, depending on the progression of the reaction).

In contrast, the LH mechanism proposes the adsorption of both reagents (methanol and glyceride) on the basic sites of the heterogeneous catalyst. The first stage corresponds to methanol and glyceride adsorption (diglyceride, monoglyceride, or glycerol, depending on the progression of the reaction). The second stage implies the chemical reaction where the tetrahedral intermediate is generated on the surface of the catalyst, where the reagents are linked to the catalyst in near sites. Finally, the corresponding methyl ester would be released in the third stage, and glyceride desorption would take place in the final stage.

The global reaction rate for transesterification with heterogeneous catalysis will depend on the reaction rate of the rate-limiting stage. Thus, the reaction time required to obtain a conversion that complies with UNE-EN standard (that is, 96.5% FAMES [8]) is always longer than the reaction time required through homogeneous catalysis, due to diffusion problems originated by the inclusion of a new phase in the reaction medium, that is, the heterogeneous catalyst. Consequently, basic heterogeneous catalysts require, in general, more extreme chemical reactions and longer reaction times than in the case of homogeneous catalysts [4].

In order to review the different research dealing with basic heterogeneous catalysts for fatty acid methyl ester production, the approach carried out by Lee et al. [9] is useful, and according to Hattori classification [10], these heterogeneous catalysts are classified in four main groups: metal oxides, zeolites, metal halides, and hydrotalcites.

Among simple metal oxides, transesterification using CaO [11–20] and MgO [7,17,21,22] has been widely researched, as both oxides are relatively cheap and present an acceptable activity. Other metal oxides have been studied, such as SrO [17,19,23], BaO [17], ZnO [19], TiO₂ [19], ZrO₂ [19], CeO₂ [24], or La₂O₃ [24].

If different simple metal oxides are compared (La₂O₃, MgO, ZnO and CeO₂), some studies pointed out that the activity of these catalysts followed this decreasing order: La₂O₃ > MgO >> ZnO~CeO₂ [24]. From these results, the authors concluded that the strength of basic active sites on the surface of catalysts is vital for the suitable development of a transesterification reaction. Consequently, regarding heterogeneous catalyst preparation, researchers have paid attention to the increase in basicity on metal oxide surfaces through chemical treatments [25] or the combination of metal oxides [26,27], which usually present high activity.

In contrast, heterogeneous basic catalysts usually present leaching processes [28], making the difference between homogeneous and heterogeneous contribution to transesterification difficult [29]. Some authors studied CaO leaching in methanol and glycerol, stating that, although CaO leaching took place, the homogeneous contribution of this catalyst was markedly lower than the heterogeneous contribution [30].

Mixed oxides, or oxides supported on other oxides, can present some advantages thanks to the strong interaction between both species. One of the most important advantages is the introduction of bifunctionality to increase the resistance of the catalyst against free fatty acids and moisture [27,31]. Therefore, saponification and neutralization reactions would be reduced. Some work studied CaO supported on different catalysts, such as SiO₂, Al₂O₃ or MgO, to increase the mechanical resistance of the catalyst and its resistance to lixiviation. The best results were obtained with CaO/MgO, and, although the catalytic properties were improved compared to the original metal oxides, the impregnation of the catalyst was needed after three cycles of use [32]. Other studies considered CaO impregna-

tion with LiNO_3 , observing that, if Li_2O were obtained after calcination, lixiviation took place, whereas if LiNO_3 was generated after calcination (instead of Li_2O), there was no homogeneous contribution [33]. Lixiviation was observed when MgO was impregnated with LiNO_3 [34].

Regarding mixed oxides, good results were obtained with the following mixtures: $\text{Al}_2\text{O}_3\text{-SnO}_2$, $\text{Al}_2\text{O}_3\text{-ZnO}$, and $\text{MgO-La}_2\text{O}_3$ [35,36]. In addition, other mixtures including an alkaline earth oxide (mainly CaO) or lanthanide oxide and a transition metal oxide (including Ti , Mn , Fe , Zr , or Ce) have been considered [37]. The catalysts with the highest resistance and durability during transesterification were CaZrO_3 and CaO-CeO_2 , being re-used five and seven times, respectively, although 10 h were required to obtain suitable conversions.

Zeolites have been used as heterogeneous catalysts for biodiesel production, whose main problem was the long reaction time required and their quick deactivation due to lixiviation or poisoning [38–41].

Other interesting catalysts are KF , KI , K_2CO_3 , and KNO_3 over Al_2O_3 . Although these catalysts have presented suitable initial results, they also present, to a greater or lesser extent, deactivation or activity loss due to lixiviation [31,42–45].

Numerous studies have been published about the use of Mg-Al as hydrotalcites [21,46–51]. Several of the most interesting characteristics of hydrotalcites are their resistance to moisture and free fatty acids, not observing lixiviation processes [21,48], and presenting a high catalytic activity when other components (such as KF , iron ions, or lithium) are added [52–55].

Although there are a lot of studies about the preparation of these catalysts and their corresponding activity, different optimum conditions have been found for every heterogeneous catalyst. Indeed, some contradictory results were found concerning the yields obtained.

Finally, the use of sustainable raw materials to produce biodiesel has been considered, looking for local crops that are adapted to local climates and offer good oil yields, with suitable properties like high oxidative stability. That is the case for rapeseed, a popular crop to produce biodiesel, especially in Europe, where its production is considerable and relatively cheap [56], which can contribute to sustainability as it is resistant to extreme climates and its production is relatively easy in many different areas (presenting resistance to extreme weather conditions and to different kind of soils). Indeed, it has been widely studied, normally under homogeneous catalysis, and the subsequent biodiesel showed good results, complying with most of the requirements of standards [57–59].

Considering the above, the aim of this work was to study biodiesel production from rapeseed oil through heterogeneous catalysis (with $\text{NaNO}_3/\text{SiAl}$). Catalyst production was carried out following similar procedures found in the literature to obtain a catalyst that is easily produced from relatively available materials. Thus, a complete characterization of the catalyst used, as well as the optimization of the chemical reaction and the characterization of the subsequent biodiesel, was carried out.

2. Materials and Methods

2.1. Catalyst Preparation

A commercial metal oxide was selected as support (silica-alumina powder, Sigma-Aldrich, St. Louis, MO, USA). As a precursor salt, NaNO_3 was selected (99.9%, Merck, Kenilworth, NJ, USA). The following steps were carried out to prepare the heterogeneous catalyst:

- Impregnation: Different NaNO_3 solutions were prepared to obtain different impregnation amounts in the final catalyst. Thus, the suitable amount of solution ($1.91 \text{ mL} \cdot \text{g}^{-1}_{\text{support}}$) was added to a certain amount of support, impregnating the latter for 2 h with a stirring rate of 200 rpm.
- Solutions were dried at 100°C .
- Activation was achieved through calcination at 600°C for 25 h. Through this technique, different metal oxides and crystals are obtained.

Thus, different samples were obtained depending on the impregnation degree ($\text{NaNO}_3/\text{SiAl } X/1$, where X is expressed in $\text{mmol}_{\text{Na}} \cdot \text{g}_{\text{support}}^{-1}$): support (SiAl),

NaNO₃/SiAl 5/1, NaNO₃/SiAl 10/1, NaNO₃/SiAl 20/1, and NaNO₃/SiAl 40/1, which were properly characterized as explained in following sections, selecting the most suitable product for transesterification optimization and the subsequent final biodiesel production.

2.2. Catalyst Characterization

2.2.1. Lixiviation Test

In order to check the reusability of the final catalyst, lixiviation tests were carried out. Thus, if lixiviation takes place, it is an undesirable effect that could indicate mechanical and chemical instability.

A certain amount of catalyst was put in contact with methanol at 65 °C for 180 min. The mixture was then centrifuged and filtered through a membrane (PTFE, 0.45 µm). Once separated, the catalyst was characterized in order to check for a possible loss of its components or properties. In contrast, the filtered methanol was used in a transesterification reaction without any catalyst (see following sections for further details about the chemical conditions), with metals included in the lixivate as the only species that can catalyze the reaction. Thus, the conversion of the oil calculated as FAME yield (calculated through gas chromatography) and the subsequent homogeneous contribution were assessed.

2.2.2. X-ray Diffraction Analysis

For mineral and structure determination, X-ray diffraction analysis (XDR) was used. Thus, a diffractometer with Bragg-Brentano geometry (Bruker D8 Advance, Billerica, MA, USA) was used, with a Ge (200) monochromator and a Vantec linear detector with an aperture of 12°, to scan from 10 to 100° (2θ). A K_{α1} radiation of Cu was used with a wavelength of 1.5406 Å. Time constant was fixed at 0.5 s, with a 2θ increase of 0.02° in the measuring range between 10 and 80° (2θ).

2.2.3. Scanning Electron Microscopy

In order to determine the morphological analysis of the heterogeneous catalysts, scanning electron microscopy (SEM) was used. For this purpose, a scanning electron microscope (Quanta 3D FEG, Houston, TX, USA) with a secondary electron detector for high vacuum (ETD) and a variable accelerating voltage was used.

2.2.4. Nitrogen Gas Adsorption-Desorption Isotherms

To determine porosity and surface area in the heterogeneous catalysts, a N₂-adsorption volumetric equipment (Quantachrome Instruments, AS-1 Series, Boynton Beach, FL, USA) was used, in a pressure range from 0 to 10,000 torr, a minimum relative pressure (P/P₀) of 3 × 10⁻⁷ torr, and 0.11% accuracy. The sample (approximately 0.3–0.5 g) was previously degasified at 250 °C for 24 h. The N₂ adsorption isotherm was obtained at the boiling point of liquid nitrogen (77 K), requiring between 90 and 150 min to achieve balance, depending on the sample. To obtain S_{BET}, 11 points were obtained at the suitable relative pressures.

2.2.5. X-ray Photoelectron Spectroscopy Analysis

To obtain information about the atomic composition (Na, O, Si, Al, C or N) in the surface of the heterogeneous catalysts, X-ray photoelectron spectroscopy (XPS) was used. The spectra were registered with a photoelectron spectrometer (K-Alpha-Thermo Scientific, Waltham, MA, USA), a monochromatic X-ray source (Al K_α at 1486.68 eV), and a perpendicular irradiation (90° at 12 kV and 6 mA). The equipment has an offset charge device through "Flood Gun", activated for every analysis in this experiment.

For complete spectra, specific conditions were used (200 eV, 50 ms for waiting time, and 1 eV for energy supply), and the atomic ratio was calculated as in Equation (1):

$$\frac{n_i}{n_j} = \frac{(I_i/S_i)}{(I_j/S_j)} \quad (1)$$

where n_i and n_j are the number of atoms per cm^3 for element i and j , respectively; I_i and I_j are the intensities corresponding to the peak of element i and j , respectively; and S_i and S_j are the sensitivity factors of element i and j , respectively.

2.2.6. Reusability Tests

In order to check the decrease in activity of the heterogeneous catalyst with ongoing use, the transesterification reaction was repeated several times (see the following section for further details), recovering the catalyst through filtration and drying. Thus, the activity of the catalyst was related to the final FAME content (through gas chromatography) obtained after transesterification.

2.3. Transesterification Reaction

2.3.1. Raw Material Used

In this case, rapeseed oil was used for transesterification, provided by the “Agrarian Research Institute Finca La Orden-Valdesequera”, belonging to CICYTEX (Centro de Investigaciones Científicas y Tecnológicas de Extremadura). The seeds were collected in the 2020 season, obtaining the corresponding oil through mechanical extraction (without any chemical treatments). The oil had free fatty acid content below 1%, and was filtered and stored in 25 L containers for further treatments.

2.3.2. Chemical Reaction

The procedure and facilities (reactor and heating and refrigeration systems) used for transesterification were explained in previous studies [60,61]. In short, 250 g of rapeseed oil was added to the reactor, adding a suitable amount of methanol, and reaching a certain temperature and stirring rate. Once the reaction medium was stabilized, a suitable amount of heterogeneous catalyst was added. The reaction was continued for 180 min. For reaction monitoring, at different reaction times 2 mL of sample was collected and filtered, cooling it down for FAME quantification through gas chromatography determination according to UNE-EN 14214 standard [8]. Thus, the activity of the catalyst was determined by transesterification yield.

2.3.3. Study of the Effect of Variables on Heterogeneous Transesterification

Different variables were considered to assess their effect on FAME production through heterogeneous catalysis:

- Catalyst amount: from 3 to 7% w/w ;
- Stirring rate: from 300 to 900 rpm;
- Methanol/oil ratio: from 6:1 to 15:1;
- Temperature: from 45 to 65 °C.

After considering effectiveness and efficiency for each variable, the optimized values were determined for the final transesterification process.

2.3.4. Kinetic Study

Once the influence of the main chemical conditions and impregnation was assessed, a kinetic study of transesterification with the selected heterogeneous catalyst was carried out.

Two models were used: Langmuir-Hinshelwood (LH) and Eley-Rideal (ER). Thus, global transesterification reaction using heterogeneous catalysis (r_h) will be given by Equations (2) (for LH) and (3) (for ER).

$$r_h = -\frac{dn_A}{dt} \cdot \frac{1}{W} = \frac{k \cdot C_A \cdot C_B}{1 + K_A \cdot C_A + K_B \cdot C_B} \quad (2)$$

$$r_h = -\frac{dn_A}{dt} \cdot \frac{1}{W} = \frac{k \cdot C_A \cdot C_B}{1 + K_B \cdot C_B} \quad (3)$$

where $-dn_A/dt$ represents the moles consumed of reagent A (triglyceride), k is the kinetic constant, W is the weight of catalyst, C_A is triglyceride concentration at a certain time t , K_A is the constant of adsorption balance for triglyceride, C_B is the concentration of B reagent (methanol) at a time t , and K_B is the constant of adsorption balance for methanol.

The global transesterification reaction can be described by Equation (4), where A represents the triglyceride molecule, B is methanol, C is fatty acid methyl ester (FAME), and D is glycerol.



Considering the relation between the concentration of reagents and their conversion and the stoichiometry of the process, Equations (5) and (6) are obtained.

$$C_A = C_{A0}(1 - X) \quad (5)$$

$$\theta_B = \frac{C_{B0}}{C_{A0}} \quad (6)$$

Substituting into Equations (2) and (3), the reaction rate based on conversion for LH Equation (7) and ER Equation (8) are obtained.

$$\frac{dX}{dt} = \frac{k \cdot (W/n_{A0}) \cdot C_{A0}^2 \cdot (1 - X) \cdot (\theta_B - 3X)}{1 + K_A \cdot C_{A0} \cdot (1 - X) + K_B \cdot C_{A0} \cdot (\theta_B - 3X)} \quad (7)$$

$$\frac{dX}{dt} = \frac{k \cdot (W/n_{A0}) \cdot C_{A0}^2 \cdot (1 - X) \cdot (\theta_B - 3X)}{1 + K_B \cdot C_{A0} \cdot (\theta_B - 3X)} \quad (8)$$

where n_{A0} represents the initial moles of A, C_{A0} and C_{B0} represent the initial concentration of A and B, respectively, and X is triglyceride conversion (A).

Once the kinetic constant and K_B are obtained for different temperatures, the activation energy (E_a) and the adsorption heat of methanol (ΔH_B) were obtained through linear regression of the Arrhenius Equation (9) and the Van't Hoff Equation (10):

$$\ln k = \ln A_0 - \frac{E_a}{R} \cdot \frac{1}{T} \quad (9)$$

$$\ln K_B = \ln K_{B0} - \frac{\Delta H_B}{R} \cdot \frac{1}{T} \quad (10)$$

2.3.5. Biodiesel Characterization

Once rapeseed biodiesel was obtained through transesterification with methanol by using the final heterogeneous catalyst and the subsequent chemical conditions, it was characterized by analyzing FAME content and profile [62], iodine value (IV) [63], density [64], viscosity [65], cold filter plugging point (CFPP) [66], acid number (AN) [67], flash point (FP), and combustion point (CP) [68]. These analyses were explained in detail in previous studies, following the corresponding standard [8].

To sum up, the main stages of this experiment are included in Figure 1.

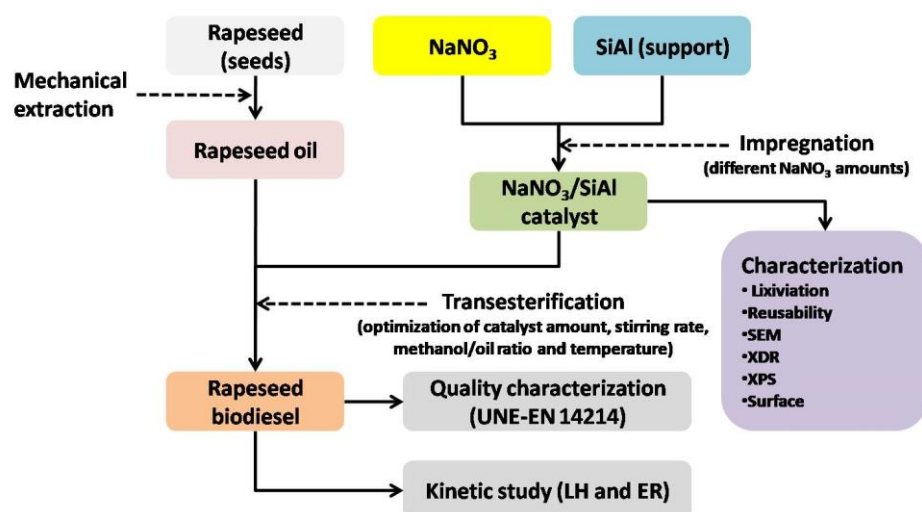


Figure 1. Experimental design.

3. Results and Discussion

3.1. Effect of Impregnation on Catalyst Preparation

SiAl was impregnated with different amounts of NaNO_3 , carrying out activity tests whose results are included in Table 1. As inferred, the support did not present any activity, whereas the increase in activity once NaNO_3 was added was not linear, reaching high FAME contents (exceeding 99%) for 20 and 40 $\text{mmol}_{\text{Na}} \cdot \text{g}_{\text{support}}^{-1}$.

Table 1. Activity tests of $\text{NaNO}_3/\text{SiAl}$ catalysts. Experimental conditions: methanol/oil ratio, 9:1; temperature, 65 °C; catalyst amount, 7% w/w; stirring rate, 700 rpm; reaction time, 180 min.

Impregnated Amount, $\text{mmol}_{\text{Na}} \cdot \text{g}_{\text{support}}^{-1}$	FAME Content, % w/w
0 ¹	0
5	<1
10	18.2
20	99.3
40	99.3

¹ In this case, the support underwent the same thermal treatment (600 °C for 25 h) without any impregnation.

Consequently, FAME lower limit according to the standard (96.5%) [8] was achieved for the highest amounts of impregnation, and $\text{NaNO}_3/\text{SiAl}$ 20/1 was selected for further analysis, as it reached the same highest activity with lower impregnated amount. Other studies confirmed similar trends, with a higher activity as the active phase increased. Thus, in the case of KOH supported on fumed silica, similar impregnation rates (30%) were considered, as it showed the highest FAME conversion from edible cooking oil [69].

3.2. Lixiviation Tests

In order to determine if this activity was due to a homogeneous contribution on account of the dilution of metal species, lixiviation tests were carried out for the selected heterogeneous catalyst, whose main results are included in Table 2.

Table 2. Lixiviation tests for NaNO₃/SiAl 20/1. Experimental conditions: temperature, 65 °C; reaction time, 180 min; stirring rate, 700 rpm.

Catalyst Amount, % w/w	Methanol/Oil Ratio	FAME Content, % w/w
Diluted species	9 ^(a) :1	3.25
7 ^(b)	9 ^(c) :1	98.8

^(a) Methanol filtered, previously put in contact with the heterogeneous catalyst. ^(b) Catalyst recovered after methanol filtration. ^(c) Pure methanol.

From this table, it can be observed that the homogeneous contribution of this catalyst was almost negligible compared to its heterogeneous contribution. Therefore, this product could be suitable for heterogeneous catalysis applied to transesterification of triglycerides with methanol.

3.3. XRD Analysis

In order to check the crystal phases of the solids, XRD analysis were carried out for the support (Si-Al) and NaNO₃/SiAl 20/1 before its use, after mixing it for 3 h with methanol and once transesterification took place. The corresponding diffractograms are included in Figure 2.

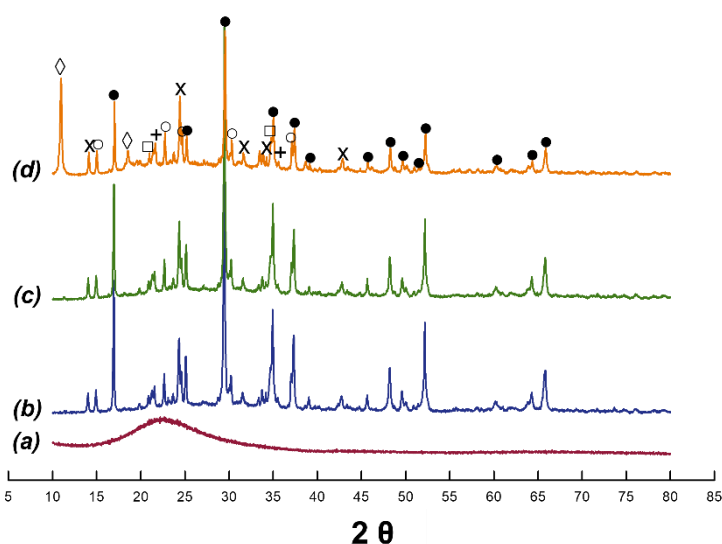


Figure 2. XRD diffractogram of NaNO₃/SiAl 20:1 catalyst: (line a) support (heat-treated SiAl); (line b) NaNO₃/SiAl 20:1 without any use; (line c) NaNO₃/SiAl 20:1 after 3 h in contact with methanol; (line d) NaNO₃/SiAl 20:1 after transesterification. Crystalline phases: + SiO₂; • Na₂SiO₃; ○ Na₂Si₂O₅; □ (NaO)₂_{0.33}NaAlSiO₄; × Na₈(AlSiO₄)₆(NO₃)₂; ◇ carbonous species.

Thus, after impregnation of the support with sodium nitrate, followed by calcination at 600 °C for 25 h, different crystal phases were obtained, with the majority species related to sodium silicates [70,71] and some sodium aluminosilicates [72,73]. All the identified species (compared to International Centre for Diffraction Data-Powder Diffraction Files) in the case of the catalyst without any use (line b in Figure 2) were also detected after its contact with methanol for 3 h (line c in Figure 2) and when it was recovered after transesterification (line d in Figure 2). This fact seems to confirm that leaching processes hardly took place and, consequently, the homogeneous catalytic contribution of the solid is negligible as expected according to the results included in Table 2. In contrast, concerning the catalyst used (line d in Figure 2), some diffraction peaks were detected, which were attributed to carbonaceous materials (not included in the catalysts without any use). This fact could indicate that some reagents, intermediate species, or products obtained during transesterification could interact with the catalyst to generate these species.

3.4. Reusability Tests of Heterogeneous Catalyst

The activity of a catalyst tends to decrease with its use due to chemical or physical factors, mainly poisoning, aging, or deactivation by coke [74]. Therefore, in this study the evolution of $\text{NaNO}_3/\text{SiAl 20/1}$ activity with successive cycles was assessed. The transesterification process was carried out several times, recovering the catalyst after each experiment (by filtering and drying at $90\text{ }^\circ\text{C}$ for 12 h). As a result, FAME contents for the four first cycles were 99.3, 98.5, 95.6, and 60.9% *w/w*, respectively. It can be inferred that deactivation did not take place for the three first cycles, whereas after the third cycle a considerable decrease in activity (above 35%) was observed. Therefore, for the fourth cycle FAME content did not comply with UNE-EN 14214 standard [8]. Other studies have pointed out, for heterogeneous catalysts such as KOH supported on fumed silica applied to transesterification reaction, similar results for the first three cycles, exceeding 99% in all cases [69].

To determine if activity loss was due to poisoning, different tests were performed to regenerate $\text{NaNO}_3/\text{SiAl 20/1}$ after the third cycle. For this purpose, different washing treatments with different solvents and the subsequent drying process were carried out (according to different studies, where the success of catalyst regeneration depended on the procedure and the studied catalyst) [31,75–77]. Figure 3 shows the main results concerning the different regeneration processes of $\text{NaNO}_3/\text{SiAl 20/1}$ catalyst, compared to the third use of this catalyst.

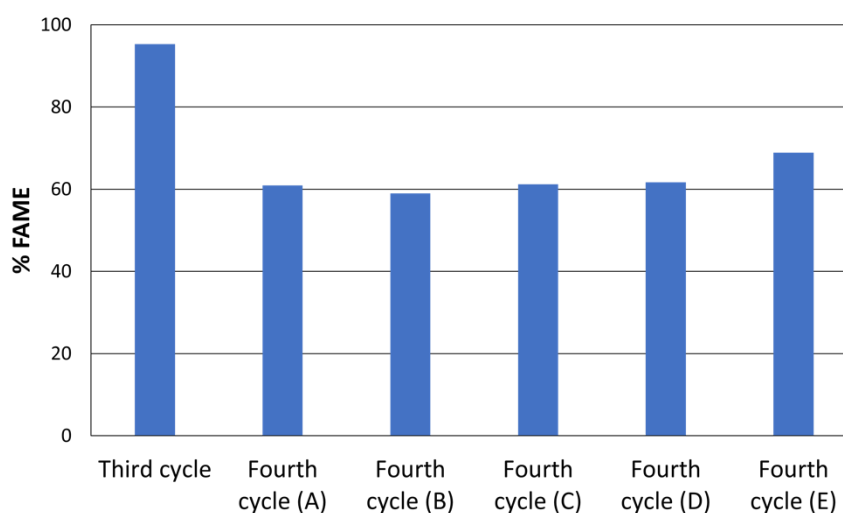


Figure 3. Study of catalyst regeneration ($\text{NaNO}_3/\text{SiAl 20/1}$) after its third use: (bar A) filtering and drying; (bar B) washing treatment (acetone) and drying; (bar C) washing treatment (methanol) and drying; (bar D) two washing treatments (methanol and heptane) and drying; (bar E) washing treatment (methanol and $\text{NH}_4\text{OH 5M}$).

According to these results, none of these washing treatments significantly improved the activity of the catalyst, as the values obtained were similar to the fourth transesterification cycle (Figure 3, bar A). Therefore, deactivation could be due to coke deposition on active sites, as observed in line d in Figure 2. Assuming this scenario, the catalyst used after three cycles was calcinated at $600\text{ }^\circ\text{C}$ for 12 h, using it afterwards in a new cycle. Again, the result of this test was like those values observed in Figure 3, with a FAME content of 61.6% *w/w*.

Thus, further studies about the causes of this deactivation are required in order to clarify if coke deposition on active sites or its basicity loss, among other factors, play an important role in this aspect.

Although an economic and easy regeneration of the catalyst was not assured, the fact that $\text{NaNO}_3/\text{SiAl 20/1}$ kept its activity for three transesterification cycles with methanol makes it a promising precursor to obtain an economic and effective catalyst for biodiesel production.

Regarding XRD, different tests were carried out depending on the quantity of sodium nitrate, with the aim of assessing the effect of the interaction between the impregnated salt and the support during the activation process (thermal treatment at 600 °C for 25 h) for the generation of different crystal phases (see Figure 2). Figure 4 shows the diffractograms for the different heterogeneous catalysts generated, with impregnations of 5, 10, 20, and 40 mmol of NaNO_3 per gram of Si-Al.

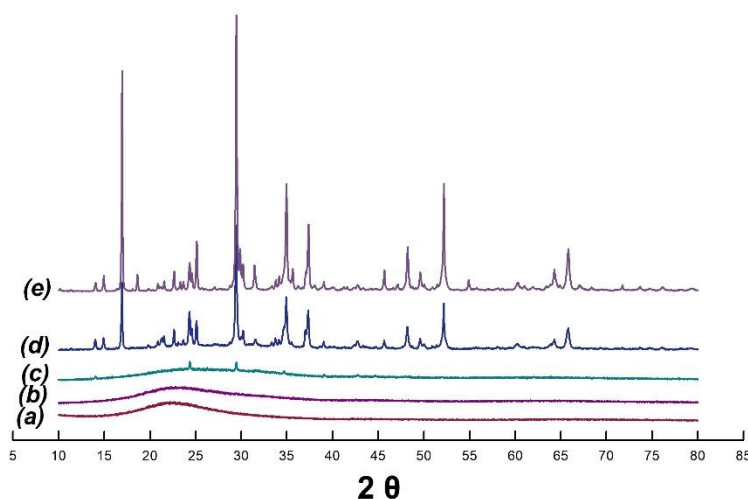


Figure 4. XRD diffractogram of $\text{NaNO}_3/\text{SiAl } x:1$: (line a) support: heat-treated SiAl; (line b) $\text{NaNO}_3/\text{SiAl } 5:1$; (line c) $\text{NaNO}_3/\text{SiAl } 10:1$; (line d) $\text{NaNO}_3/\text{SiAl } 20:1$; (line e) $\text{NaNO}_3/\text{SiAl } 40:1$.

As observed, the crystal phases changed as the amount of sodium nitrate increased. In that sense, the diffractograms of the support and $\text{NaNO}_3/\text{SiAl } 5:1$ were practically the same (lines a and b in Figure 4), without any clear crystal phase being observed. For $\text{NaNO}_3/\text{SiAl } 10:1$ (line c in Figure 4), small diffraction peaks were observed, possibly due to $\text{Na}_8(\text{AlSiO}_4)_6(\text{NO}_3)_2$ [73] and Na_2SiO_3 [70]. Finally, for $\text{NaNO}_3/\text{SiAl } 20:1$ and $\text{NaNO}_3/\text{SiAl } 40:1$ (lines d and e in Figure 4), the diffraction peaks were clearly observed, related to the crystal phases noted in Figure 2.

These results were linked to FAME content obtained when different impregnated amounts were used (see Table 1). When $\text{NaNO}_3/\text{SiAl } 5:1$ was used (solid with an identical diffractogram compared to the support), conversion was not observed. With $\text{NaNO}_3/\text{SiAl } 10:1$ (where some crystal phases were detected), conversion reached 18% *w/w* and, finally, when $\text{NaNO}_3/\text{SiAl } 20:1$ and $\text{NaNO}_3/\text{SiAl } 40:1$ were used (with complex diffractograms with at least four crystal phases detected), conversion exceeded 99% *w/w*.

3.5. SEM Analysis

The morphological analysis of the support (SiAl) and the selected catalyst ($\text{NaNO}_3/\text{SiAl } 20:1$) was carried out through scanning electron microscopy (SEM). The most representative images are included in Figures 5 and 6.

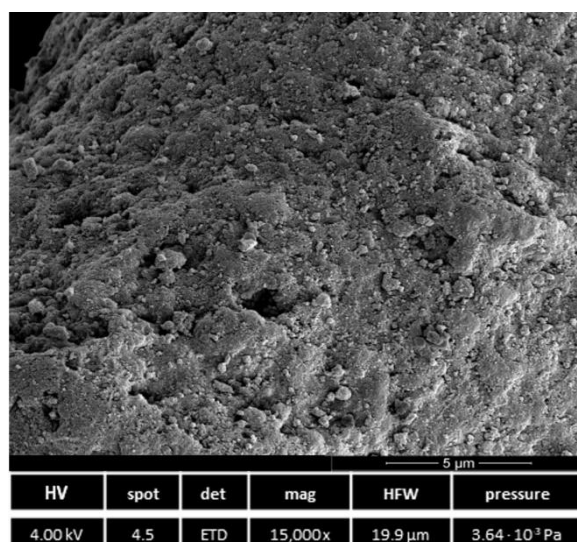


Figure 5. Micrograph obtained through SEM of the catalyst support (SiAl) after thermal treatment (600 °C for 25 h).

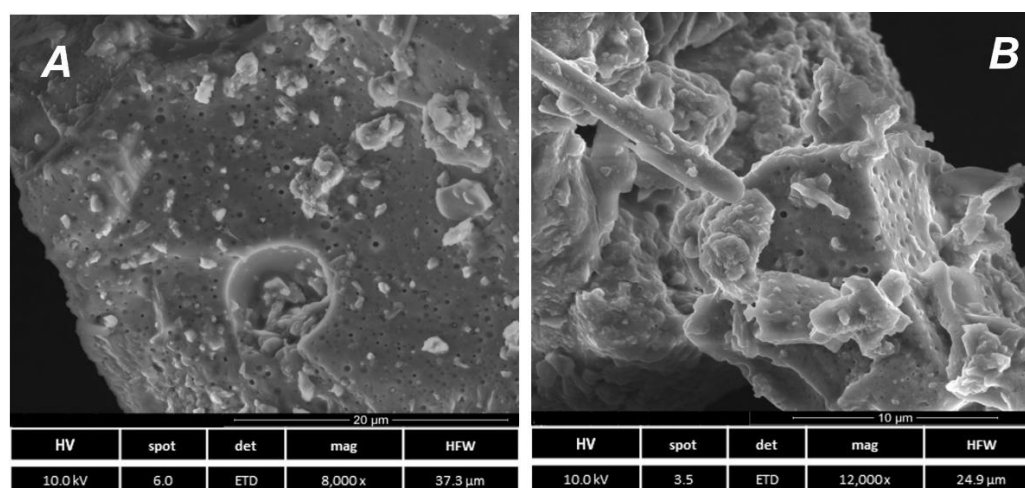


Figure 6. Micrographs obtained through SEM of the catalyst (NaNO₃/SiAl 20/1) at different magnifications: 8000 times (A) and 12,000 times (B).

As observed in the case of the support, its surface was uniform, without any defined crystal. Nevertheless, if this solid is compared to NaNO₃/SiAl 20/1 (Figure 6), clear differences were observed, as there were crystals of different sizes on the surface of the catalyst.

Therefore, it can be said that the surface of the catalyst was heterogeneous, with crystal agglomerations of different shapes and sizes, which were unevenly distributed on its surface (see Figure 6A). The presence of agglomerations (as observed in Figure 6B) is typical in this kind of heterogeneous catalyst, as confirmed by other authors once the final catalyst was obtained (as in the case of alumina supported coconut chaff), possibly due to the aggregation of small particles during catalyst preparation [78]. The detailed analysis of the obtained micrographs showed a higher compaction of the surface, possibly due to crystal agglomeration. In addition, the apparent porosity of the catalyst did not have inner extension, remaining as closed holes.

3.6. Surface Analysis

The results concerning S_{BET} determination through the analysis of nitrogen adsorption isotherms are included in Table 3.

Table 3. Specific surface of support and catalysts (depending on impregnation).

Sample	SiAl ¹ (Support)	NaNO ₃ /SiAl x/1			
		5/1	10/1	20/1	40/1
S _{BET} , m ² ·g ⁻¹	448.2	1.522	0.410	1.238	2.406

¹ The support underwent the same thermal treatment (600 °C, 25 h).

There was a drastic decrease in specific surface for the catalysts, compared to the support, regardless the amount of sodium nitrate used for impregnation. This could be due to a strong sintering effect when the nitrate salt was put in contact with the support during the thermal treatment. Other studies, where the support (fumed silica) was impregnated with increasing amounts of KOH, showed a similar trend, with a drastic decrease in specific surface once impregnation took place, possibly on account of the fact that the pores of the support were filled or the potassium species were deposited on the pore openings [69].

Nevertheless, as inferred from Table 1, the activity of the catalyst was high although the specific surface was low. This fact could indicate that some of the crystal phases generated with higher amounts of sodium nitrate could be responsible for this activity.

3.7. XPS Analysis

In order to assess the crystal phases or species that present a high catalytic activity in the catalysts, X-ray photoelectron spectroscopy (XPS) was carried out. Thus, the surface quantification and atomic ratios, obtained according to previous studies [79], are included in Table 4.

Table 4. Surface quantification and atomic ratio for support and catalysts.

	SiAl	NaNO ₃ /SiAl x/1			
		5/1	10/1	20/1	40/1
Na 1s	n.d. ¹	9.20	14.01	20.48	25.40
O 1s	59.98	53.74	53.39	49.94	47.10
Si 2p	32.60	25.92	21.62	16.30	14.14
Al 2p	5.66	4.49	3.86	2.76	3.22
C 1s	1.76	6.64	5.73	9.39	9.49
N 1s	n.d.	n.d.	1.38	1.13	0.65
Atomic ratios Na/Si/Al	0/85.8/14.2	15.2/71.9/12.9	23.4/65.0/11.6	35.5/52.0/10.5	47.2/42.8/10.0

¹ Not determined.

As inferred from the diffractograms included in Figure 4, as the amount of impregnation increased, Na₂SiO₃ presented a higher increase in signal peaks, which implies a higher amount of this species compared to others. However, after the atomic percentage determination of Na and Si on the surface of the catalysts through XPS, the Na/Si ratio did not reach a value of 2:1 (corresponding to Na₂SiO₃). This fact could indicate that the crystal phases with less relative amount of Na (such as Na₂Si₂O₅) could be in the most superficial areas of the catalyst, being, therefore, responsible for the high catalytic activity of the catalyst.

In contrast, Table 5 includes the results obtained through XPS for NaNO₃/SiAl 20/1 without any use, in contact with methanol and after a transesterification reaction.

Table 5. Surface quantification and atomic ratios through XPS for NaNO₃/SiAl 20/1 without any use, in contact with methanol and after a transesterification reaction.

Species, %	Without Use	Methanol Contact	After Transesterification
Na 1s	20.48	22.48	7.27
O 1s	49.94	46.73	19.15
Si 2p	16.30	11.52	2.64
Al 2p	2.76	4.34	1.09
C 1s	9.39	14.93	69.86
N 1s	1.13	n.d. ¹	n.d.
Atomic ratios Na/Si/Al	35.5/52.0/10.5	41.6/46.9/11.5	50.4/30.2/19.4

¹ Not determined.

There was an increase in C atoms on the catalyst surface when it was used (compared to the catalyst without any use), in accordance with the diffraction peaks due to carbonaceous matter (see Figure 2), which accumulated on catalytic sites, decreasing catalytic activity. Regarding the atomic ratios, when the catalyst was put in contact with methanol and, especially, when it was used in a transesterification reaction, the Si ratio decreased whereas Na and Al ratios increased. This fact, along with C increase, could indicate that the active centers of the catalysts are facilitated by Si atoms (these active points are possibly basic sites associated with O), and coke could be generated around these sites. Consequently, Si could be hidden from XPS analysis, and the decrease observed in the table would not be a real loss (that is, Si is not properly revealed by using this technique).

3.8. Influence of Variables during Transesterification

Once the activity of the final heterogeneous catalyst NaNO₃/SiAl 20/1 was confirmed and its characterization was carried out, the study of the influence of the main variables affecting transesterification (of rapeseed oil with methanol through heterogeneous catalysis) was attempted.

Regarding catalyst addition (see Figure 7A), there was a considerable increase in FAME production from 3 to 5% *w/w*, but not from 5 to 7% *w/w*, reaching the same conversion at the end of the experiment. When the latter amounts were used, high conversions (99.3% *w/w*), like those observed for homogeneous catalysis [80,81], were seen. Concerning the influence of the amount of catalyst on reaction rate, there was an initial induction period for all the experiments (for approximately 15–20 min), as observed in previous studies for KNO₃ over CaO [82]. This period could result from two factors: the adsorption stage of the reagents (which is a characteristic of heterogeneous catalysis) and diffusion phenomena between the existing phases in the first stage of the reaction mechanism (liquid-liquid system due to triglycerides and methanol). In contrast, an increase in reaction rate was observed as the amount of catalyst increased (as in the case of other homogeneous and heterogeneous catalysts [82,83]), although the highest differences were obtained between 3 and 5% *w/w*. Equally, for 3% the conversion was lower (91.3%) compared to 5 and 7% *w/w*, requiring longer reaction times for the former.

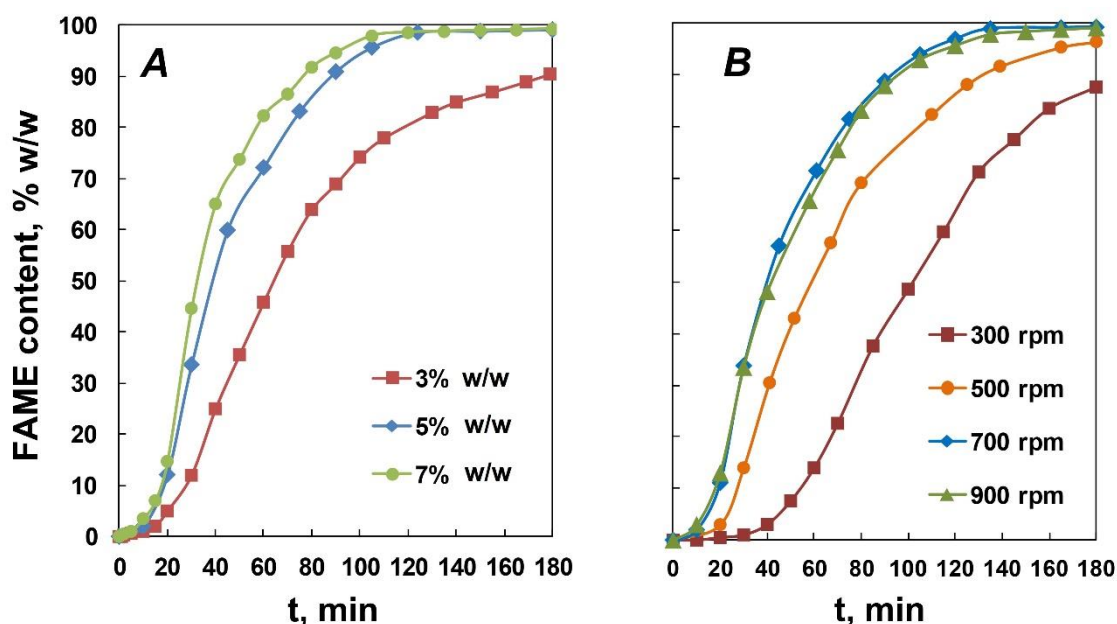


Figure 7. Effect of: (A) catalyst concentration (stirring rate = 700 rpm, $T = 65\text{ }^{\circ}\text{C}$, ratio = 9:1, time = 180 min) and (B) stirring rate ([Catalyst] = 5%, $T = 65\text{ }^{\circ}\text{C}$, ratio = 9:1, time = 180 min) on FAME production.

Considering these results, 5% *w/w* was selected for the study of the remaining parameters, as higher amounts of catalyst did not significantly increase the reaction rate nor FAME production.

Considering that in the case of transesterification through heterogeneous catalysis, a three-phase system takes place (solid-liquid-liquid), global reaction rate could be influenced by reagent adsorption on catalyst surface, the diffusion of the reagents between the phases, or desorption of products from the surface. With the aim of assessing which stage is prevalent, the stirring rate was studied. Different stirring rates (from 300 to 900 rpm) were tested, keeping the rest of the operating variables constant, as observed in Figure 7B.

A strong influence of stirring rate on reaction rate was observed up to 700 rpm. Concerning the initial induction period, it was longer as the stirring rate decreased, although it did not completely disappear at the highest values. The fact that stirring rates exceeding 700 rpm had similar profiles could indicate that, under these chemical conditions, the global reaction rate of the process is not controlled by diffusion phenomena. Considering these results, the stirring rate selected for further studies was 700 rpm.

As is known, the use of methanol/oil ratios higher than the stoichiometric one favors the shift of the chemical balance towards product generation, that is, FAME or biodiesel. As it is difficult to obtain high FAME conversions from the stoichiometric ratio, higher ratios are needed in order to comply with the standard [1,84]. Surplus methanol could be re-used, which would not imply further costs at the industrial scale. Methanol/oil ratio is one of the most influential factors on reaction rate and yield, and its optimum value is usually related to the kind of catalyst used, among other reaction conditions (kind of reactor, temperature, etc.) [3,85]. In this experiment, different ratios were used, from 6:1 to 15:1, keeping the remaining parameters constant, as illustrated in Figure 8A. As inferred from this figure, conversion and reaction rate were similar, regardless the ratio, when it exceeded 9:1. On the contrary, lower ratios showed long induction periods and subsequent low conversion percentages after 3 h (83% for 6:1 methanol/oil ratio). This could be because, regardless the mechanism used (Rideal or Langmuir-Hinshelwood), both situations imply methanol adsorption on the catalyst surface, a process that is influenced by the increase in this reagent until all the active sites of the catalyst are covered. For further analysis, and considering these results, the methanol/oil ratio selected was 9:1.

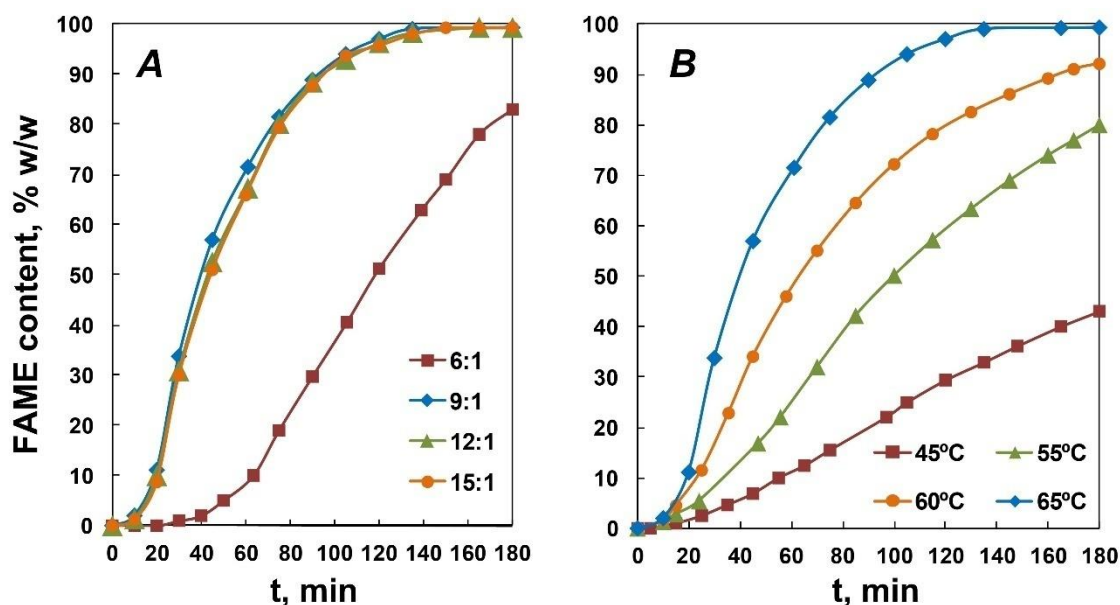


Figure 8. Effect of: (A) methanol/oil ratio ([Catalyst] = 5%, T = 65 °C, stirring rate = 700 rpm, time = 180 min) and (B) temperature ([Catalyst] = 5%, stirring rate = 700 rpm, ratio = 9:1, time = 180 min) on FAME production.

Regarding temperature, different tests were carried out, from 45 to 65 °C and keeping the remaining parameters constant (see Figure 8B).

As observed, there was a strong influence on the duration of the initial induction period and the reaction rate. As expected, as the global transesterification reaction is an endothermal chemical balance, the reaction rate to generate FAMEs was influenced by the increase in reaction temperature [82]. In addition, as the transesterification process through heterogeneous catalysis is slower compared to the corresponding homogeneous catalysis, the positive effect of temperature is more pronounced. Concerning FAME content, only at 65 °C was the chemical balance reached, with a constant conversion from 120 min. Thus, this was the selected temperature for further analysis.

3.9. Kinetic Study

Once the study of the main variables of the process (affecting transesterification of rapeseed oil with methanol and using $\text{NaNO}_3/\text{SiAl } 20/1$) was completed, the kinetic study of the process was conducted. The following approaches were considered:

- The homogeneous catalysis contribution of the catalyst was negligible, as experimentally proved in this experiment.
- The external diffusion of the reagents from the liquid phase to the surface of the solid does not control the global reaction rate if the stirring rate is at least 700 rpm.
- In the time range considered for the kinetic study (once the induction point ended), the global reaction rate was influenced by the chemical reaction on the surface of the catalyst. As a consequence, both reagent adsorption and product desorption, as well as inner diffusion, do not affect the global reaction rate of the process.
- For this same time range, the catalyst distribution is homogeneous in the reaction medium for a methanol/oil ratio of 9:1 or higher.
- There is no weight loss of the catalyst and, therefore, it does not take part in any secondary reaction of the process.

With these approaches and considering kinetic studies about heterogeneous catalysis found in the literature, the following kinetic models were used: Langmuir-Hinshelwood (LH) [6,7], where both triglycerides and methanol are adsorbed on active sites of the catalyst; and Eley-Rideal (ER) [5,6] assuming that only methanol is adsorbed.

Once the kinetic equations were defined (see Section 2), the experimental data were adjusted (data obtained for experiments included in Figure 7A, where different amounts of catalysts were studied at constant temperature, stirring rate, and methanol/oil ratio), obtaining the results included in Table 6.

Table 6. Kinetic parameters for LH and ER models for different catalyst additions. Experimental conditions: methanol/oil ratio, 9:1; temperature, 65 °C; stirring rate, 700 rpm.

Catalyst Addition	3% w/w	5% w/w	7% w/w
	W = 7.5 g	W = 12.5 g	W = 17.5 g
	$n_{A0} = 0.2753 \text{ mol}$ $C_{A0} = 0.7306 \text{ M}$ $\theta_B = 9.2931$		
Model	Langmuir-Hinshelwood		
Kinetic parameters	$k = 2.333 \times 10^{-3} \text{ L}^2 \cdot \text{g}_{\text{cat}}^{-1} \cdot \text{mol}^{-1} \cdot \text{min}^{-1}$ $K_A = 6.3 \times 10^{-23} \text{ L} \cdot \text{mol}^{-1}$ $K_B = 2.071 \text{ L} \cdot \text{mol}^{-1}$		
R ²	0.9992	0.9989	0.9996
S	0.0157	0.0235	0.0164
Model	Eley-Rideal		
Kinetic parameters	$k = 2.333 \times 10^{-3} \text{ L}^2 \cdot \text{g}_{\text{cat}}^{-1} \cdot \text{mol}^{-1} \cdot \text{min}^{-1}$ $K_B = 2.071 \text{ L} \cdot \text{mol}^{-1}$		
R ²	0.9992	0.9989	0.0006
S	0.0157	0.0236	0.0163

As observed, the experimental data were satisfactorily adjusted to both models, with a coefficient of determination close to one and low standard deviation values.

The low K_A value obtained (near 0) could indicate that the LH model could be simplified to obtain the ER model. That is the reason why the latter had similar adjustment values, with k and K_B values that are practically identical to those found in the LH model. Some authors also found that ER was more suitable to reproduce the results found for the transesterification of ethyl acetate with methanol, using MgO as a catalyst [7]. Similarly, other studies successfully used this model in the kinetic study of palm oil transesterification with methanol, using KF/Ca-Mg-Al as a heterogeneous catalyst [86].

Considering the above, in order to study the influence of temperature on reaction rate during transesterification through heterogeneous catalysis (by using NaNO₃/SiAl 20/1), the experimental data corresponding to Figure 8B were selected, adjusted for the ER model. Table 7 shows the main results.

Table 7. Kinetic parameters by using the ER model at different reaction temperatures. Experimental conditions: catalyst addition, 5% w/w; methanol/oil ratio, 9:1; stirring rate: 700 rpm.

	$n_{A0} = 0.2753 \text{ mol}$	$C_{A0} = 0.7306 \text{ M}$	$\theta_B = 9.2931$	
	45 °C	55 °C	60 °C	65 °C
$k \cdot 10^{-3} (\text{L}^2 \cdot \text{g}_{\text{cat}}^{-1} \cdot \text{mol}^{-1} \cdot \text{min}^{-1})$	0.432	1.001	1.354	2.333
$K_B (\text{L} \cdot \text{mol}^{-1})$	2.49	2.30	2.18	2.07
R ²	0.9992	0.9998	0.9996	0.9989
s	0.0179	0.0177	0.0098	0.0236

Considering the values of the kinetic constant (k) and the balance constant in the case of methanol adsorption (K_B) for each temperature, the activation energy of the process (E_a) and the adsorption heat for methanol (ΔH_B) were calculated, through the Arrhenius and Van't Hoff logarithmic equations.

The adjustments of k and K_B at different temperatures (Table 7) to the aforementioned equations are included in Figure 9.

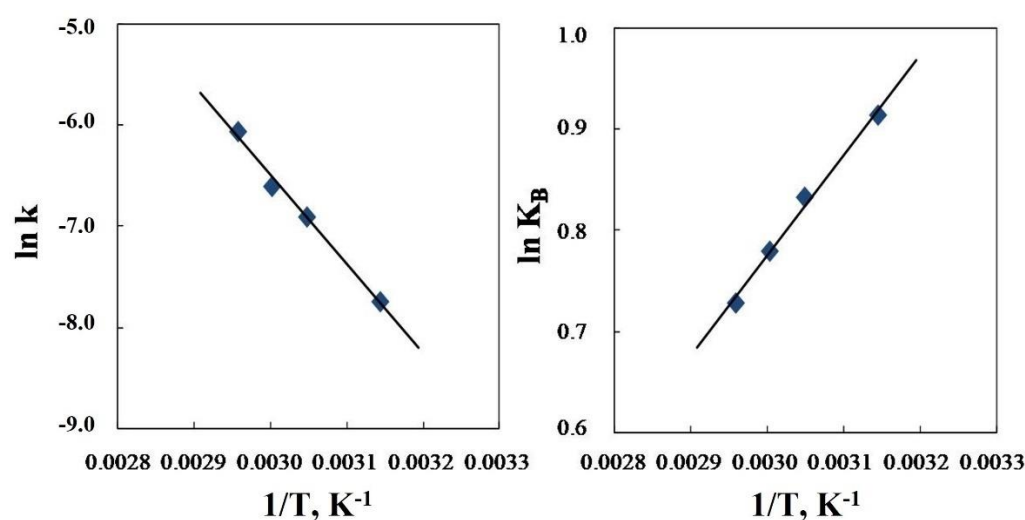


Figure 9. Influence of temperature on transesterification kinetics by using $\text{NaNO}_3/\text{SiAl 20/1}$. Linear adjustment through Arrhenius (left) and Van't Hoff (right).

According to these methods, the activation energy and adsorption heat obtained are shown in Table 8.

Table 8. Activation energy and methanol adsorption heat through the adjustment to Arrhenius and Van't Hoff equations. Comparison with the literature.

Reference (Catalyst)	Arrhenius		Van't Hoff	
	E_a ($\text{kJ}\cdot\text{mol}^{-1}$)	A_0 ($\text{L}^2\cdot\text{g}_{\text{cat}}^{-1}\cdot\text{mol}^{-1}\cdot\text{min}^{-1}$)	E_a ($\text{kJ}\cdot\text{mol}^{-1}$)	A_0 ($\text{L}^2\cdot\text{g}_{\text{cat}}^{-1}\cdot\text{mol}^{-1}\cdot\text{min}^{-1}$)
$\text{NaNO}_3/\text{SiAl 20/1}$ R^2	73.3	4.6×10^8 0.992	−8.28	0.109 0.992
$\text{KF}/\text{Ca-Mg-Al}$ [86] R^2	109.6	1.4×10^{14} 0.967	−36.2	1.2×10^{-6} 0.906
$\text{Ca}(\text{C}_3\text{H}_7\text{O}_3)_2/\text{CaCO}_3$ [57] R^2	42.5	372.4 0.999 ¹	n.d. ²	n.d. n.d.

¹ Adjustment from two k values experimentally determined. ² Not determined.

As observed, the activation energy obtained in this experiment ($73.3 \text{ kJ}\cdot\text{mol}^{-1}$) was within the same range compared to other heterogeneous catalysts. The adsorption heat obtained for methanol was negative, which is typical, in general, in this kind of process (normally exothermic) [82].

Figure 10 shows the theoretical and experimental evolution of this experiment through the ER model (considering E_a , A_0 , K_{B0} , and ΔH_B obtained in Tables 7 and 8) for some transesterification experiments carried out through basic heterogeneous catalysis with $\text{NaNO}_3/\text{SiAl 20/1}$. According to this figure and considering the good correlation coefficients obtained for the ER model, the latter suitably reproduced the experimental data. However, it should be considered that this model is suitable once the induction period ended, which could imply that the reaction is controlled by mass transfer at the early stages. Once the substance is adsorbed on the catalyst, the process would be controlled by the chemical reaction that takes place on the surface. That is the reason why this model would not be suitable for low heating rates or methanol/oil ratios (below 700 rpm or 9:1, respectively).

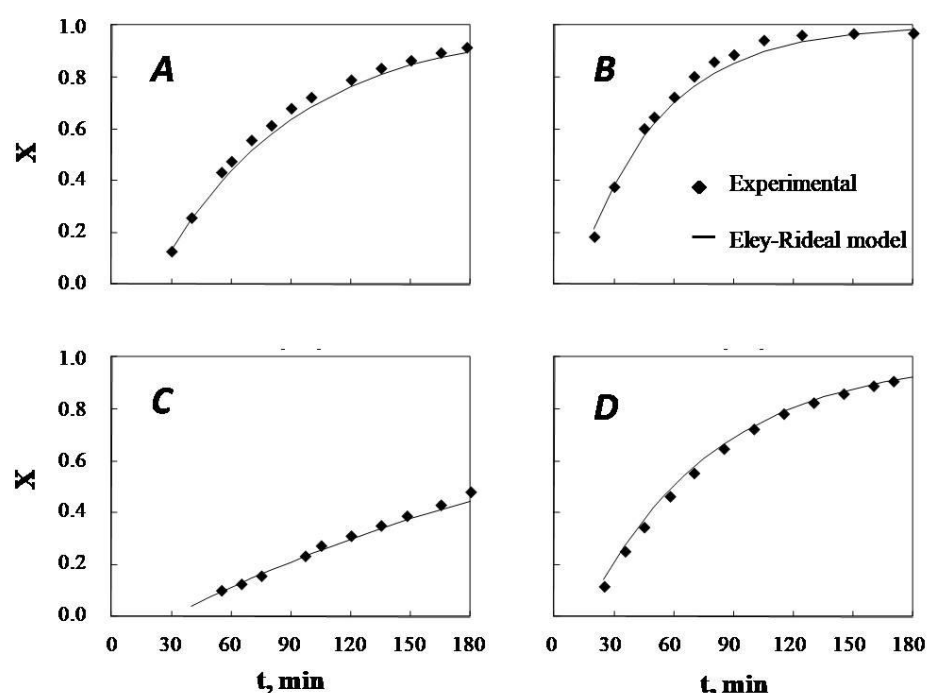


Figure 10. Conversion of FAMEs with reaction time: comparison between experimental and theoretical data (according to Eley-Rideal method). Chemical conditions for each experiment: (A) catalyst amount, 3% w/w; methanol/oil ratio, 9:1; stirring rate, 700 rpm; temperature, 65 °C; (B) catalyst amount, 5% w/w; methanol/oil ratio, 9:1; stirring rate, 700 rpm; temperature, 65 °C; (C) catalyst amount, 5% w/w; methanol/oil ratio, 9:1; stirring rate, 700 rpm; temperature, 45 °C; (D) catalyst amount, 5% w/w; methanol/oil ratio, 9:1; stirring rate, 700 rpm; temperature, 60 °C.

3.10. FAME Quality Determination

Finally, the quality of the biodiesel (that is, FAMEs) obtained under the selected chemical conditions (catalyst amount, 5% w/w; methanol/oil ratio, 9:1; stirring rate, 700 rpm; temperature, 65 °C) was assessed. After a characterization according to UNE-EN 14214 standard, the main results are included in Table 9.

Table 9. Quality parameters of rapeseed biodiesel through heterogeneous catalysis ($\text{NaNO}_3/\text{SiAl } 20/1$) with methanol.

FAME Profile	C14:0	C16:0	C16:1	C18:0	C18:1	C18:2	C18:3	C22:0
% w/w	0.04	4.19	0.19	1.50	66.6	17.2	7.71	<0.01
Parameter	FAME %	IV $\text{g}_{12} \cdot 100 \text{ g}^{-1}$	Density $\text{g} \cdot \text{L}^{-1}$	Viscosity cSt	CFPP °C	AN $\text{mg}_{\text{KOH}} \cdot \text{g}^{-1}$	FP °C	CP °C
	99.3	101.3	879	4.43	−7	0.28	175	190

According to this table, it can be inferred that, as expected, the kind of catalyst did not considerably influence the quality of biodiesel, as similar results were comparing homogeneous and heterogeneous catalysis for rapeseed biodiesel [57,82,83]. Thus, conversion is important and determines the final quality of biodiesel, with high yields assuring compliance with most parameters included in standards [8].

4. Conclusions

The most important findings inferred from this work were the following:

- The preparation of heterogeneous catalysts supported on SiAl through impregnation with NaNO_3 , followed by calcination (600 °C for 25 h), lead to catalysts ($\text{NaNO}_3/\text{SiAl}$) with high activity. Their activity increased with $\text{NaNO}_3/\text{SiAl}$ ratio, and 99.3% FAMEs

were obtained with a ratio of 20/1 (NaNO₃/SiAl 20/1). Its activity during the transesterification of rapeseed oil was maintained during the first three cycles, considerably decreasing its activity in subsequent cycles.

- The generation of silicate and aluminosilicate crystals in the heterogeneous catalysts was confirmed through XRD. There was an almost complete loss of S_{BET} compared to the surface of the support, which could indicate the development of strong sintering processes during the preparation of the catalyst. The catalyst had a very heterogeneous surface, with crystal agglomeration and low porosity according to S_{BET} analysis.
- Regarding the influence of variables on rapeseed oil transesterification by using NaNO₃/SiAl 20/1, it can be concluded that higher values of the following parameters had almost no positive effect on reaction rate and effectiveness: amount of catalyst (5% w/w), methanol/oil ratio (9:1), and stirring rate (700 rpm). In contrast, temperature had a clear positive effect on kinetics.
- The use of the Eley-Rideal adsorption-reaction model properly predicted the transesterification kinetics studied in this case. At 65 °C, the reaction rate constant (k) and adsorption constant for methanol (K_B) were 2.33·10⁻³ L²·g_{cat}⁻¹·mol⁻¹·min⁻¹ and 2.071 L mol⁻¹, respectively. The activation energy (E_a) and adsorption molar heat for methanol (ΔH_B) were 73.3 kJ·mol⁻¹ and -8.28 kJ·mol⁻¹, respectively.
- Finally, the properties of the biodiesel obtained under these circumstances, compared to basic homogeneous catalysis, were practically identical. Therefore, the properties of biodiesel depended on FAME content and distribution, regardless the process used to obtain it.

Author Contributions: Conceptualization, J.M.E. and J.F.G.; methodology, J.M.E., J.F.G. and G.M.; validation, J.M.E. and G.M.; formal analysis, G.M.; investigation, J.M.E. and G.M.; resources, J.M.E. and J.F.G.; data curation, G.M. and S.N.-D.; writing—original draft preparation, S.N.-D.; writing—review and editing, S.N.-D.; visualization, J.M.E. and J.F.G.; supervision, J.M.E., J.F.G. and S.N.-D.; project administration, J.M.E. and J.F.G.; funding acquisition, J.M.E. and J.F.G. All authors have read and agreed to the published version of the manuscript.

Funding: This research was funded by Junta de Extremadura and FEDER, grant numbers GR18150 and IB18028.

Acknowledgments: Now, when we have less time left for the end, J. M. Encinar would like to thank the “little help from my friends” (which is immaterial, but very important). Thanks to Blas, María José “la de Diego”, Manolo, Petri, Félix, Diego, Marisol, Ana (who, apart from being my friend, is my wife), Toni, María José “la de Toni”, Dolores, Riqui and María Luisa. Thank you so much for sharing our lives. Also, the authors would like to acknowledge the economic support provided by Junta de Extremadura and FEDER (GR18150 and IB18028).

Conflicts of Interest: The authors declare no conflict of interest.

References

1. Rodionova, M.V.; Poudyal, R.S.; Tiwari, I.; Voloshin, R.A.; Zharmukhamedov, S.K.; Nam, H.G.; Zayadan, B.K.; Bruce, B.D.; Hou, H.J.M.; Allakhverdiev, S.I. Biofuel production: Challenges and opportunities. *Int. J. Hydrogen Energy* **2017**, *42*, 8450–8461. [[CrossRef](#)]
2. MacLeod, C.S.; Harvey, A.P.; Lee, A.F.; Wilson, K. Evaluation of the activity and stability of alkali-doped metal oxide catalysts for application to an intensified method of biodiesel production. *Chem. Eng. J.* **2008**, *135*, 63–70. [[CrossRef](#)]
3. Rizwanul Fattah, I.M.; Ong, H.C.; Mahlia, T.M.I.; Mofijur, M.; Silitonga, A.S.; Ashrafur Rahman, S.M.; Ahmad, A. State of the Art of Catalysts for Biodiesel Production. *Front. Energy Res.* **2020**, *8*, 1–17. [[CrossRef](#)]
4. Nisar, S.; Hanif, M.A.; Rashid, U.; Hanif, A.; Akhtar, M.N.; Ngamcharussrivichai, C. Trends in widely used catalysts for fatty acid methyl esters (Fame) production: A review. *Catalysts* **2021**, *11*, 1085. [[CrossRef](#)]
5. Di Serio, M.; Tesser, R.; Pengmei, L.; Santacesaria, E. Heterogeneous Catalysts for Biodiesel Production. *Energy Fuels* **2008**, *22*, 207–217. [[CrossRef](#)]
6. Endalew, A.K.; Kiros, Y.; Zanzi, R. Inorganic heterogeneous catalysts for biodiesel production from vegetable oils. *Biomass Bioenergy* **2011**, *35*, 3787–3809. [[CrossRef](#)]
7. Dossin, T.; Reyniers, M.; Marin, G. Kinetics of heterogeneously MgO-catalyzed transesterification. *Appl. Catal. B Environ.* **2006**, *62*, 35–45. [[CrossRef](#)]

8. UNE-EN 14214:2013 V2+A1:2018. *Liquid Petroleum Products—Fatty Acid Methyl Esters (FAME) for Use in Diesel Engines and Heating Applications—Requirements and Test Methods*; Asociación Española de Normalización: Madrid, Spain, 2018.
9. Lee, D.-W.; Park, Y.-M.; Lee, K.-Y. Heterogeneous Base Catalysts for Transesterification in Biodiesel Synthesis. *Catal. Surv. Asia* **2009**, *13*, 63–77. [[CrossRef](#)]
10. Hattori, H. Solid Base Catalysts: Generation, Characterization, and Catalytic Behavior of Basic Sites. *J. Jpn. Pet. Inst.* **2004**, *47*, 67–81. [[CrossRef](#)]
11. Gryglewicz, S. Rapeseed oil methyl esters preparation using heterogeneous catalysts. *Bioresour. Technol.* **1999**, *70*, 249–253. [[CrossRef](#)]
12. Watkins, R.S.; Lee, A.F.; Wilson, K. Li–CaO catalysed tri-glyceride transesterification for biodiesel applications. *Green Chem.* **2004**, *6*, 335–340. [[CrossRef](#)]
13. Granados, M.L.; Poves, M.D.Z.; Alonso, D.M.; Mariscal, R.; Galisteo, F.C.; Moreno-Tost, R.; Santamaría, J.; Fierro, J.L.G. Biodiesel from sunflower oil by using activated calcium oxide. *Appl. Catal. B Environ.* **2007**, *73*, 317–326. [[CrossRef](#)]
14. Liu, X.; He, H.; Wang, Y.; Zhu, S.; Piao, X. Transesterification of soybean oil to biodiesel using CaO as a solid base catalyst. *Fuel* **2008**, *87*, 216–221. [[CrossRef](#)]
15. Kouzu, M.; Kasuno, T.; Tajika, M.; Sugimoto, Y.; Yamanaka, S.; Hidaka, J. Calcium oxide as a solid base catalyst for transesterification of soybean oil and its application to biodiesel production. *Fuel* **2008**, *87*, 2798–2806. [[CrossRef](#)]
16. Veljković, V.B.; Stamenković, O.S.; Todorović, Z.B.; Lazić, M.L.; Skala, D.U. Kinetics of sunflower oil methanolysis catalyzed by calcium oxide. *Fuel* **2009**, *88*, 1554–1562. [[CrossRef](#)]
17. Patil, P.; Gude, V.G.; Pinappu, S.; Deng, S. Transesterification kinetics of Camelina sativa oil on metal oxide catalysts under conventional and microwave heating conditions. *Chem. Eng. J.* **2011**, *168*, 1296–1300. [[CrossRef](#)]
18. Yoosuk, B.; Udomsap, P.; Puttasawat, B.; Krasae, P. Improving transesterification activity of CaO with hydration technique. *Bioresour. Technol.* **2010**, *101*, 3784–3786. [[CrossRef](#)]
19. Yoo, S.J.; Lee, H.; Veriansyah, B.; Kim, J.; Kim, J.-D.; Lee, Y.-W. Synthesis of biodiesel from rapeseed oil using supercritical methanol with metal oxide catalysts. *Bioresour. Technol.* **2010**, *101*, 8686–8689. [[CrossRef](#)]
20. Mazaheri, H.; Ong, H.C.; Amini, Z.; Masjuki, H.H.; Mofijur, M.; Su, C.H.; Badruddin, I.A.; Yunus Khan, T.M. An overview of biodiesel production via calcium oxide based catalysts: Current state and perspective. *Energies* **2021**, *14*, 3950. [[CrossRef](#)]
21. Di Serio, M.; Ledda, M.; Cozzolino, M.; Minutillo, G.; Tesser, R.; Santacesaria, E. Transesterification of Soybean Oil to Biodiesel by Using Heterogeneous Basic Catalysts. *Ind. Eng. Chem. Res.* **2006**, *45*, 3009–3014. [[CrossRef](#)]
22. Wang, L.; Yang, J. Transesterification of soybean oil with nano-MgO or not in supercritical and subcritical methanol. *Fuel* **2007**, *86*, 328–333. [[CrossRef](#)]
23. Liu, X.; He, H.; Wang, Y.; Zhu, S. Transesterification of soybean oil to biodiesel using SrO as a solid base catalyst. *Catal. Commun.* **2007**, *8*, 1107–1111. [[CrossRef](#)]
24. Bancquart, S.; Vanhove, C.; Pouilloux, Y.; Barrault, J. Glycerol transesterification with methyl stearate over solid basic catalysts. *Appl. Catal. A Gen.* **2001**, *218*, 1–11. [[CrossRef](#)]
25. Zhu, H.; Wu, Z.; Chen, Y.; Zhang, P.; Duan, S.; Liu, X.; Mao, Z. Preparation of Biodiesel Catalyzed by Solid Super Base of Calcium Oxide and Its Refining Process. *Chin. J. Catal.* **2006**, *27*, 391–396. [[CrossRef](#)]
26. Li, X.; Lu, G.; Guo, Y.; Guo, Y.; Wang, Y.; Zhang, Z.; Liu, X.; Wang, Y. A novel solid superbase of $\text{Eu}_2\text{O}_3/\text{Al}_2\text{O}_3$ and its catalytic performance for the transesterification of soybean oil to biodiesel. *Catal. Commun.* **2007**, *8*, 1969–1972. [[CrossRef](#)]
27. Yan, S.; Kim, M.; Salley, S.O.; Ng, K.Y.S. Oil transesterification over calcium oxides modified with lanthanum. *Appl. Catal. A Gen.* **2009**, *360*, 163–170. [[CrossRef](#)]
28. Di Serio, M.; Tesser, R.; Casale, L.; D’Angelo, A.; Trifuoggi, M.; Santacesaria, E. Heterogeneous Catalysis in Biodiesel Production: The Influence of Leaching. *Top. Catal.* **2010**, *53*, 811–819. [[CrossRef](#)]
29. Sánchez Faba, E.M.; Ferrero, G.O.; Dias, J.M.; Eimer, G.A. Alternative raw materials to produce biodiesel through alkaline heterogeneous catalysis. *Catalysts* **2019**, *9*, 690. [[CrossRef](#)]
30. Granados, M.L.; Alonso, D.M.; Sádaba, I.; Mariscal, R.; Ocón, P. Leaching and homogeneous contribution in liquid phase reaction catalysed by solids: The case of triglycerides methanolysis using CaO. *Appl. Catal. B Environ.* **2009**, *89*, 265–272. [[CrossRef](#)]
31. Sharma, Y.C.; Singh, B.; Korstad, J. Latest developments on application of heterogenous basic catalysts for an efficient and eco friendly synthesis of biodiesel: A review. *Fuel* **2011**, *90*, 1309–1324. [[CrossRef](#)]
32. Yan, S.; Lu, H.; Liang, B. Supported CaO Catalysts Used in the Transesterification of Rapeseed Oil for the Purpose of Biodiesel Production. *Energy Fuels* **2008**, *22*, 646–651. [[CrossRef](#)]
33. Alonso, D.M.; Mariscal, R.; Granados, M.L.; Maireles-Torres, P. Biodiesel preparation using Li/CaO catalysts: Activation process and homogeneous contribution. *Catal. Today* **2009**, *143*, 167–171. [[CrossRef](#)]
34. Wen, Z.; Yu, X.; Tu, S.-T.; Yan, J.; Dahlquist, E. Synthesis of biodiesel from vegetable oil with methanol catalyzed by Li-doped magnesium oxide catalysts. *Appl. Energy* **2010**, *87*, 743–748. [[CrossRef](#)]
35. Macedo, C.C.S.; Abreu, F.R.; Tavares, A.P.; Alves, M.B.; Zara, L.F.; Rubim, J.C.; Suarez, P.A.Z. New heterogeneous metal-oxides based catalyst for vegetable oil trans-esterification. *J. Braz. Chem. Soc.* **2006**, *17*, S0103–S50532006000700014. [[CrossRef](#)]
36. Babu, N.S.; Sree, R.; Prasad, P.S.S.; Lingaiah, N. Room-Temperature Transesterification of Edible and Nonedible Oils Using a Heterogeneous Strong Basic Mg/La Catalyst. *Energy Fuels* **2008**, *22*, 1965–1971. [[CrossRef](#)]

37. Kawashima, A.; Matsubara, K.; Honda, K. Development of heterogeneous base catalysts for biodiesel production. *Bioresour. Technol.* **2008**, *99*, 3439–3443. [[CrossRef](#)] [[PubMed](#)]
38. Leclercq, E.; Finiels, A.; Moreau, C. Transesterification of rapeseed oil in the presence of basic zeolites and related solid catalysts. *J. Am. Oil Chem. Soc.* **2001**, *78*, 1161–1165. [[CrossRef](#)]
39. Suppes, G.J.; Dasari, M.A.; Daskocil, E.J.; Mandiky, P.J.; Goff, M.J. Transesterification of soybean oil with zeolite and metal catalysts. *Appl. Catal. A Gen.* **2004**, *257*, 213–223. [[CrossRef](#)]
40. Xie, W.; Huang, X.; Li, H. Soybean oil methyl esters preparation using NaX zeolites loaded with KOH as a heterogeneous catalyst. *Bioresour. Technol.* **2007**, *98*, 936–939. [[CrossRef](#)] [[PubMed](#)]
41. Fattahi, N.; Triantafyllidis, K.; Luque, R.; Ramazani, A. Zeolite-Based Catalysts: A Valuable Approach toward Ester Bond Formation. *Catalysts* **2019**, *9*, 758. [[CrossRef](#)]
42. Ebiura, T.; Echizen, T.; Ishikawa, A.; Murai, K.; Baba, T. Selective transesterification of triolein with methanol to methyl oleate and glycerol using alumina loaded with alkali metal salt as a solid-base catalyst. *Appl. Catal. A Gen.* **2005**, *283*, 111–116. [[CrossRef](#)]
43. Xie, W.; Peng, H.; Chen, L. Transesterification of soybean oil catalyzed by potassium loaded on alumina as a solid-base catalyst. *Appl. Catal. A Gen.* **2006**, *300*, 67–74. [[CrossRef](#)]
44. Vyas, A.P.; Subrahmanyam, N.; Patel, P.A. Production of biodiesel through transesterification of Jatropha oil using $\text{KNO}_3/\text{Al}_2\text{O}_3$ solid catalyst. *Fuel* **2009**, *88*, 625–628. [[CrossRef](#)]
45. Xie, W.; Li, H. Alumina-supported potassium iodide as a heterogeneous catalyst for biodiesel production from soybean oil. *J. Mol. Catal. A Chem.* **2006**, *255*, 1–9. [[CrossRef](#)]
46. Xie, W.; Peng, H.; Chen, L. Calcined Mg–Al hydrotalcites as solid base catalysts for methanolysis of soybean oil. *J. Mol. Catal. A Chem.* **2006**, *246*, 24–32. [[CrossRef](#)]
47. Silva, C.C.C.M.; Ribeiro, N.F.P.; Souza, M.M.V.M.; Aranda, D.A.G. Biodiesel production from soybean oil and methanol using hydrotalcites as catalyst. *Fuel Process. Technol.* **2010**, *91*, 205–210. [[CrossRef](#)]
48. Liu, Y.; Lotero, E.; Goodwin, J.G.; Mo, X. Transesterification of poultry fat with methanol using Mg–Al hydrotalcite derived catalysts. *Appl. Catal. A Gen.* **2007**, *331*, 138–148. [[CrossRef](#)]
49. Zeng, H.; Feng, Z.; Deng, X.; Li, Y. Activation of Mg–Al hydrotalcite catalysts for transesterification of rape oil. *Fuel* **2008**, *87*, 3071–3076. [[CrossRef](#)]
50. Navajas, A.; Campo, I.; Arzamendi, G.; Hernández, W.Y.; Bobadilla, L.F.; Centeno, M.A.; Odriozola, J.A.; Gandía, L.M. Synthesis of biodiesel from the methanolysis of sunflower oil using PURAL[®] Mg–Al hydrotalcites as catalyst precursors. *Appl. Catal. B Environ.* **2010**, *100*, 299–309. [[CrossRef](#)]
51. Barakos, N.; Pasiadis, S.; Papayannakos, N. Transesterification of triglycerides in high and low quality oil feeds over an HT2 hydrotalcite catalyst. *Bioresour. Technol.* **2008**, *99*, 5037–5042. [[CrossRef](#)]
52. Gao, L.; Xu, B.; Xiao, G.; Lv, J. Transesterification of Palm Oil with Methanol to Biodiesel over a KF/Hydrotalcite Solid Catalyst. *Energy Fuels* **2008**, *22*, 3531–3535. [[CrossRef](#)]
53. Gao, L.; Teng, G.; Lv, J.; Xiao, G. Biodiesel Synthesis Catalyzed by the KF/Ca–Mg–Al Hydrotalcite Base Catalyst. *Energy Fuels* **2010**, *24*, 646–651. [[CrossRef](#)]
54. Macala, G.S.; Robertson, A.W.; Johnson, C.L.; Day, Z.B.; Lewis, R.S.; White, M.G.; Iretskii, A.V.; Ford, P.C. Transesterification Catalysts from Iron Doped Hydrotalcite-like Precursors: Solid Bases for Biodiesel Production. *Catal. Lett.* **2008**, *122*, 205–209. [[CrossRef](#)]
55. Shumaker, J.L.; Crofcheck, C.; Tackett, S.A.; Santillan-Jimenez, E.; Morgan, T.; Ji, Y.; Crocker, M.; Toops, T.J. Biodiesel synthesis using calcined layered double hydroxide catalysts. *Appl. Catal. B Environ.* **2008**, *82*, 120–130. [[CrossRef](#)]
56. Jahiril, M.I.; Brown, R.J.; Senadeera, W.; O’Hara, I.M.; Ristovski, Z.D. The use of artificial neural networks for identifying sustainable biodiesel feedstocks. *Energies* **2013**, *6*, 3764–3806. [[CrossRef](#)]
57. Encinar, J.M.; González, J.F. Biodiesel and biolubricant production from different vegetable oils through transesterification. *Eng. Rep.* **2020**, *2*, 12190. [[CrossRef](#)]
58. Fernández-Tirado, F.; Parra-López, C.; Romero-Gámez, M. Life cycle assessment of biodiesel in Spain: Comparing the environmental sustainability of Spanish production versus Argentinean imports. *Energy Sustain. Dev.* **2016**, *33*, 36–52. [[CrossRef](#)]
59. Szabados, G.; Bereczky, Á. Experimental investigation of physicochemical properties of diesel, biodiesel and TBK-biodiesel fuels and combustion and emission analysis in CI internal combustion engine. *Renew. Energy* **2018**, *121*, 568–578. [[CrossRef](#)]
60. Nogales-Delgado, S.; Encinar, J.M.; González, J.F. Safflower biodiesel: Improvement of its oxidative stability by using BHA and TBHQ. *Energies* **2019**, *12*, 1940. [[CrossRef](#)]
61. Nogales-Delgado, S.; Sánchez, N.; Encinar, J.M. Valorization of cynara Cardunculus, L. Oil as the basis of a biorefinery for biodiesel and biolubricant production. *Energies* **2020**, *13*, 5085. [[CrossRef](#)]
62. UNE-EN 14112. *Fat and Oil Derivatives—Fatty Acid Methyl Esters (FAME)—Determination of Oxidation Stability (Accelerated Oxidation Test)*; Asociación Española de Normalización: Madrid, Spain, 2017.
63. UNE-EN 14111:2003. *Fat and Oil Derivatives. Fatty Acid Methyl Esters (FAME). Determination of Iodine Value*; Asociación Española de Normalización: Madrid, Spain, 2003.
64. UNE-EN-ISO 3675. *Crude Petroleum and Liquid Petroleum Products. Laboratory Determination of Density. Hydrometer Method*; Asociación Española de Normalización: Madrid, Spain, 1999.

65. UNE-EN ISO 3104/AC:1999. *Petroleum Products. Transparent and Opaque Liquids. Determination of Kinematic Viscosity and Calculation of Dynamic Viscosity (ISO 3104:1994)*; Asociación Española de Normalización: Madrid, Spain, 1999.
66. UNE-EN 116:2015. *Diesel and Domestic Heating Fuels—Determination of Cold Filter Plugging Point- Stepwise Cooling Bath Method*; Asociación Española de Normalización: Madrid, Spain, 2015.
67. UNE-EN 14104:2003. *Oil and Fat Derivatives. Fatty Acid Methyl Esters (FAME). Determination of Acid Value*; Asociación Española de Normalización: Madrid, Spain, 2003.
68. UNE-EN 51023:1990. *Petroleum Products. Determination of Flash and Fire Points. Cleveland Open Cup Method*; Asociación Española de Normalización: Madrid, Spain, 1990.
69. Ishak, N.; Estephane, J.; Dahdah, E.; Chalouhi, L.M.; Nassreddine, S.; El Khoury, B.; Aouad, S. Outstanding activity of a biodiesel coated K2O/fumed silica catalyst in the transesterification reaction. *J. Environ. Chem. Eng.* **2021**, *9*, 104665. [[CrossRef](#)]
70. International Centre for Diffraction Data. Powder diffraction file: Na₂SiO₃ Cmc 21 PDF:01-072-0079, ICDD-PDF-2. 2010.
71. International Centre for Diffraction Data. Powder diffraction file: Na₂Si₂O₅ P21/a PDF:00-023-0529, ICDD-PDF-2. 2010.
72. International Centre for Diffraction Data. Powder diffraction file: (Na₂O)_{0.33}NaAlSiO₄ F-43m PDF:00-039-0101, ICDD-PDF-2. 2010.
73. International Centre for Diffraction Data. Powder diffraction file: Na₈(AlSiO₄)₆(NO₃)₂ P-43n PDF:00-039-0101, ICDD-PDF-2. 2010.
74. González Velasco, J.R.; González Marcos, J.A.; González Marcos, M.P.; Gutiérrez Ortiz, M.A. *Cinética Química Aplicada*; Editorial Síntesis S. A.: Madrid, Spain, 1999; ISBN 8477386668.
75. Ngamcharussrivichai, C.; Totarat, P.; Bunyakiat, K. Ca and Zn mixed oxide as a heterogeneous base catalyst for transesterification of palm kernel oil. *Appl. Catal. A Gen.* **2008**, *341*, 77–85. [[CrossRef](#)]
76. Alonso, D.M.; Mariscal, R.; Moreno-Tost, R.; Poves, M.D.Z.; Granados, M.L. Potassium leaching during triglyceride transesterification using K/γ-Al₂O₃ catalysts. *Catal. Commun.* **2007**, *8*, 2074–2080. [[CrossRef](#)]
77. Di Serio, M.; Mallardo, S.; Carotenuto, G.; Tesser, R.; Santacesaria, E. Mg/Al hydrotalcite catalyst for biodiesel production in continuous packed bed reactors. *Catal. Today* **2012**, *195*, 54–58. [[CrossRef](#)]
78. Yusuff, A.S.; Owolabi, J.O. Synthesis and characterization of alumina supported coconut chaff catalyst for biodiesel production from waste frying oil. *South Afr. J. Chem. Eng.* **2019**, *30*, 42–49. [[CrossRef](#)]
79. Wagner, C.D.; Davis, L.E.; Zeller, M.V.; Taylor, J.A.; Raymond, R.H.; Gale, L.H. Empirical atomic sensitivity factors for quantitative analysis by electron spectroscopy for chemical analysis. *Surf. Interface Anal.* **1981**, *3*, 211–225. [[CrossRef](#)]
80. Koutsouki, A.A.; Tegou, E.; Badeka, A.; Kontakos, S.; Pomonis, P.J.; Kontominas, M.G. In situ and conventional transesterification of rapeseeds for biodiesel production: The effect of direct sonication. *Ind. Crops Prod.* **2016**, *84*, 399–407. [[CrossRef](#)]
81. Encinar, J.M.; González, J.F.; Pardal, A.; Martínez, G. Rape oil transesterification over heterogeneous catalysts. *Fuel Process. Technol.* **2010**, *91*, 1530–1536. [[CrossRef](#)]
82. Encinar, J.M.; Pardal, A.; Martínez, G. Transesterification of rapeseed oil in subcritical methanol conditions. *Fuel Process. Technol.* **2012**, *94*, 40–46. [[CrossRef](#)]
83. Rathore, V.; Newalkar, B.L.; Badoni, R.P. Processing of vegetable oil for biofuel production through conventional and non-conventional routes. *Energy Sustain. Dev.* **2016**, *31*, 24–49. [[CrossRef](#)]
84. Aransiola, E.F.; Ojumu, T.V.; Oyekola, O.O.; Madzimbamuto, T.F.; Ikhu-Omoregbe, D.I.O. A review of current technology for biodiesel production: State of the art. *Biomass Bioenergy* **2014**, *61*, 27–297. [[CrossRef](#)]
85. Xiao, Y.; Gao, L.; Xiao, G.; Lv, J. Kinetics of the Transesterification Reaction Catalyzed by Solid Base in a Fixed-Bed Reactor. *Energy Fuels* **2010**, *24*, 5829–5833. [[CrossRef](#)]
86. Hsieh, L.-S.; Kumar, U.; Wu, J.C.S. Continuous production of biodiesel in a packed-bed reactor using shell-core structural Ca(C₃H₇O₃)₂/CaCO₃ catalyst. *Chem. Eng. J.* **2010**, *158*, 250–256. [[CrossRef](#)]